



# Large-scale carbonate platform development of Cay Sal Bank, Bahamas, and implications for associated reef geomorphology



Sam Purkis<sup>a,\*</sup>, Jeremy Kerr<sup>a</sup>, Alexandra Dempsey<sup>a</sup>, Andrew Calhoun<sup>a</sup>, Liisa Metsamaa<sup>a</sup>, Bernhard Riegl<sup>a</sup>, Villy Kourafalou<sup>b</sup>, Andrew Bruckner<sup>c</sup>, Philip Renaud<sup>c</sup>

<sup>a</sup> National Coral Reef Institute, Nova Southeastern University, Dania Beach, FL 33004, USA

<sup>b</sup> University of Miami, Rosenstiel School of Marine and Atmospheric Science, Miami, FL 33149, USA

<sup>c</sup> Living Oceans Foundation, Landover, MD 20785, USA

## ARTICLE INFO

### Article history:

Received 31 August 2012

Received in revised form 22 September 2013

Accepted 2 March 2014

Available online 11 March 2014

### Keywords:

Carbonate platform

Geomorphology

Bahamas

Karst

Sea level

## ABSTRACT

The Bahama Archipelago consists of an arcuate chain of carbonate platforms. Average water depths on the platform-tops, such as the Great Bahama Bank (GBB), are typically 10 m or less, with coral reef-rimmed margins, thick sediment accumulations, and the frequent occurrence of islands. There are, however, exceptions. For example, Cay Sal Bank (CSB), a little studied detached Bahamian carbonate platform with depths ranging from 30 to 7 m, is only slightly deeper than the GBB, but devoid of islands, lacks platform-margin coral reefs and holds little sediment on the platform-top; the platform is incipiently drowned. CSB is interesting as it is conspicuously larger (6000 sq. km) than other incipiently drowned platforms in the region, such as Serranilla Bank (1100 sq. km) and the Cat Island platform (1500 sq. km). Field and remote sensing data are assembled to provide insight into the sedimentology and geomorphology of the CSB. The influence of ocean climate, regional hydrodynamics, and Holocene flooding history are investigated to understand why platform-margin coral reef growth on CSB has been unable to keep pace with Holocene sea-level rise. A decade of regional sea-surface temperature data for the Bahamas report CSB to be situated in the same ocean climate regime as GBB. Temperature cannot explain the platform's different morphologies. The Florida Current has been evoked as a possible reason for the immature development of platform-top processes on the CSB, but numeric modeling suggests its influence to be restricted to the deep flanks of the bank. Further, sediment distribution on CSB, including infill patterns of karst depressions, suggest trade winds (easterlies) to drive platform-top hydrodynamics. By assembling a satellite-derived bathymetry map, it can be shown that CSB flooded earlier and at relatively higher rates of Holocene sea-level rise than its neighboring platforms. Flooding history is identified as the most feasible explanation for the atypical morphology of the CSB. By contrasting the present-day morphology of the CSB and the GBB, the work emphasizes how subtle differences in relative sea-level history can influence the growth of platform-margin coral reefs, features that in turn can conspire to set even closely neighboring carbonate platforms on divergent paths with regard to the development of marine landforms. This insight is relevant to interpreting the morphological diversity of carbonate platforms in the modern ocean and in the rock record.

© 2014 Elsevier B.V. All rights reserved.

## 1. Introduction

The margins of most carbonate platforms are characterized by platform-edge reefs. However, the margins of the Cay Sal Bank (CSB) in the Bahamas are not. These margins lie in water depths of 15 m to 30 m, beneath the zone of maximum carbonate production (<10 m) (Schlager, 1981). In contrast to the neighboring Great and Little Bahama Bank (GBB and LBB), the margins of CSB are non-aggraded (lack platform-edge reefs). Neumann and Macintyre (1985) coined the

geological term “give-up” reefs to describe the scenario where changing environmental conditions, such as the decrease in light levels due to sea-level rise, serve to turn off carbonate production. Reef building on the periphery of CSB can be described as either having “given-up” or in the process of doing so. The margins of the platform are “non-aggraded”. Using the terms of Neumann and Macintyre (1985), the margins of GBB and LBB, in contrast to the CSB, are rimmed by “keep-up” reefs that initiated as soon as the platform was flooded and accreted at a similar rate as sea-level rise. The margins of these platforms are “aggraded”.

Hypotheses evoking ocean climate and Holocene flooding history have been proposed to explain why the reefs on the platform-edge of CSB have “given-up” (e.g. Hine and Steinmetz, 1984). These hypotheses,

\* Corresponding author.

E-mail address: [purkis@nova.edu](mailto:purkis@nova.edu) (S. Purkis).

and others pertaining to hydrodynamics, will be investigated in light of a recent airborne-, satellite-, and field-survey of the CSB. The dataset consists of sediment samples, acoustic subbottom profiles, several million bathymetry soundings, and SCUBA observations, all of which have been assembled in a GIS atop a validated habitat map of the platform derived from Worldview-2 satellite imagery.

Goldberg (1983) was the first to describe the marine communities of the CSB and theorized the biological impoverishment to be related to the platform's open and poorly developed reef rim. Hine and Steinmetz (1984) examined the sedimentology of CSB, noted the immature development of normal bank-top processes and facies, as well as the absence of key modern depositional environments, and hypothesized the rate of platform inundation by rising Holocene sea level to be responsible.

The aims of the study are threefold. First, to build upon Goldberg (1983) and Hine and Steinmetz (1984) and provide new insight into this little studied, but large, Bahamas isolated carbonate platform. Second, to investigate why CSB's margins are inactive and impoverished, unlike those of nearby GBB. And finally, to examine the intimate connection that is apparent between the configuration of Modern depositional environments and landforms that can be traced back to the Pleistocene and Early Holocene when the platform-top was subaerially exposed. The latter is achievable because the majority of the CSB is covered by little to no sediment.

## 2. Regional setting

Located between south Florida and Cuba, CSB is a 6000 sq. km isolated carbonate platform in the territory of the Bahamas (Fig. 1). Average water depth across the platform-top is 12 m (but variable) and the CSB's position in the central Florida Straits, within the path of the Florida Current, is a high energy setting in terms of oceanic currents, trade winds, and hurricane tracks.

Holocene sea-level history for the Straits of Florida is well constrained by Toscano and Macintyre (2003) who present a carefully compiled sea-level curve bracketed between corals and peat. The CSB lies within the overall study area of Toscano and Macintyre (2003) and rates of Holocene sea-level rise can be inferred from their data up until 11,000 years BP (before present) and from Alley et al. (2005) from 11,000 to 12,000 years BP. Average subsidence rate of the nearby Great Bahama Bank is in the range of 0.02 m/ka (Pierson, 1982) which can be considered broadly equivalent to that of the CSB (Hine and Steinmetz, 1984).

## 3. Quantitative methods

A one month field campaign to study the CSB was conducted in May 2011 aboard the Motor Yacht Golden Shadow, a 67-meter logistical support vessel. In excess of five million single-beam depth soundings and approximately 50 km of digital geophysical profiles were obtained with a 5 kHz SyQwest Stratabox subbottom profiler, all integrated with a Differential Global Positioning System (DGPS) and mounted on a 10 m day boat. All soundings and subbottom profiles were normalized to chart datum (lowest astronomical tide). Seabed video was collected at 580 sites using a tethered SeaViewer video camera, also integrated with the DGPS (Fig. 2).

Digital subbottom profiler data were processed using The Kingdom Suite (v. 7.5) seismic interpretation software. The first stage of processing consisted of detrending and correcting for geometrical spreading. A "swell" filter was then applied (following Haynes et al., 1997) to remove the effects of the ~0.3 m amplitude water-wave motion present at the time of survey. Application of the filter resulted in a marked enhancement of the lateral continuity of the subsurface layering. Inspection of subbottom profiles enabled a description of the morphology and topography of both the Holocene sediments and the Pleistocene carbonate platform on which they have been deposited.

Surficial sediment samples (each 500 mL in volume) were collected at 90 stations across the platform-top using a semi-random sampling strategy based on environments determined from the Worldview-2 (WV2) satellite imagery (Fig. 3). Sedimentary facies description from the WV2 was paired with grain-size and grain-shape analyses of the sediment samples using a Camsizer (Retsch and Co. KG), a compact laboratory instrument that utilizes digital imaging technology for the analysis of incoherent materials in the range of 30  $\mu\text{m}$  to 30 mm (4 phi to -4 phi). Ten of the 90 samples were randomly selected and sieved to validate the grain-size distributions obtained from the Camsizer. No difference was observed between the two methods. The Camsizer data were interpolated to a 100  $\times$  100 m grid to provide insight into the distribution of grain-size across the platform-top of CSB.

### 3.1. Satellite mapping of seabed habitats

This study employs DigitalGlobe WV2 satellite data to image the platform-top of CSB. Comparison of contrast-stretched WV2 images with UKHO nautical charts and single-beam soundings indicate the deepest areas where seabed character could be discerned correspond to a water depth of 40 m, which is consistent with visible light

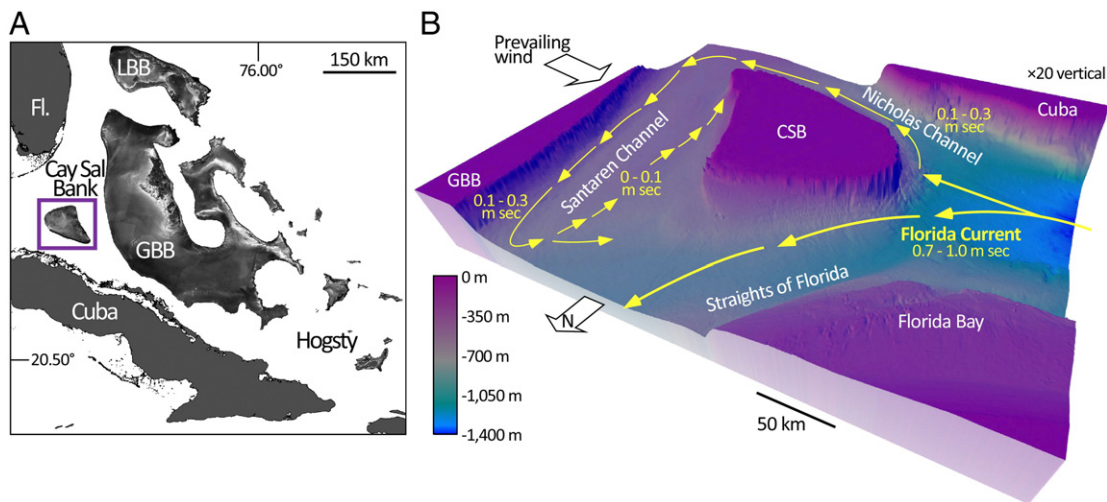


**Fig. 1.** A) The Cay Sal Bank (CSB) is a 6000 sq. km isolated carbonate platform located between south Florida, Cuba, Great Bahama Bank (GBB) and Little Bahama Bank (LBB). B) Seafloor morphology of CSB based on National Ocean Service Hydrographic Survey Data. Current vectors and rates of flow (arrows) generalized from the Florida Straits, South Florida and Florida Keys Hybrid Coordinate Ocean Model (FKeys-HYCOM) – Kourafalou and Kang (2012).

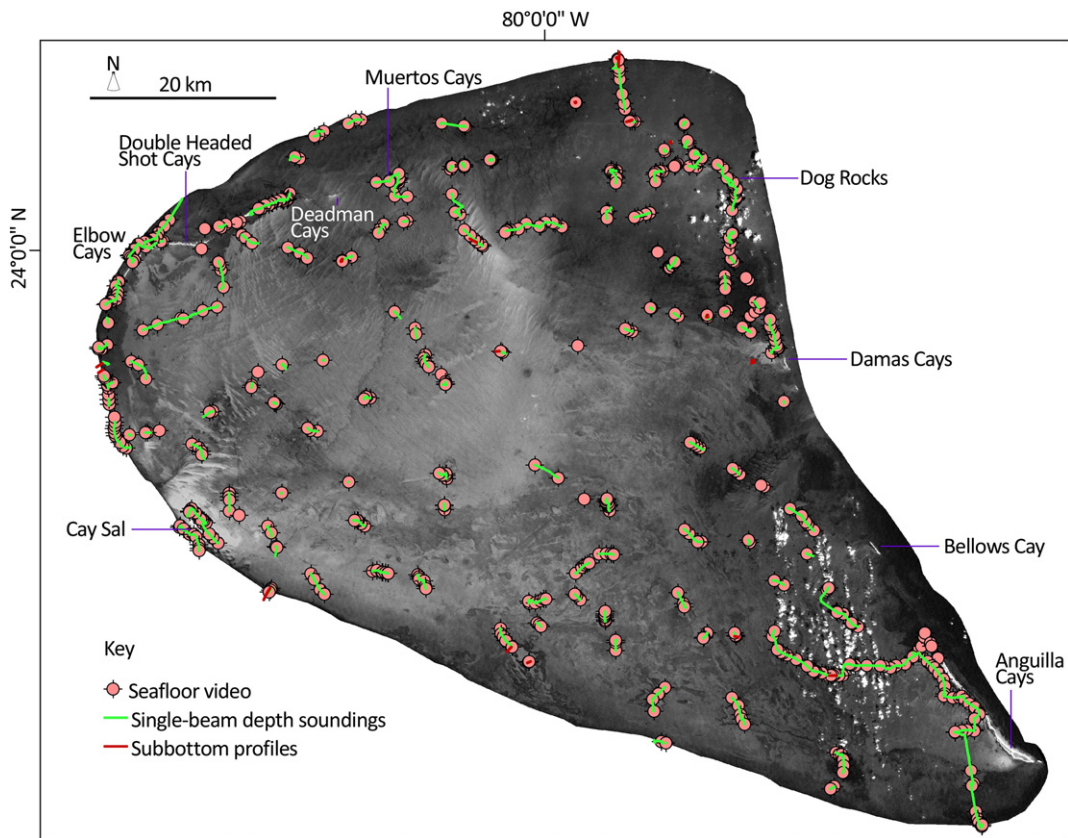


**Fig. 2.** Locations of seabed video, single-beam bathymetric soundings, and subbottom profiles superimposed on a grayscale Landsat image of the Cay Sal Bank. Emergent Cays are labeled. Credit: Landsat courtesy of U.S. Geological Survey.

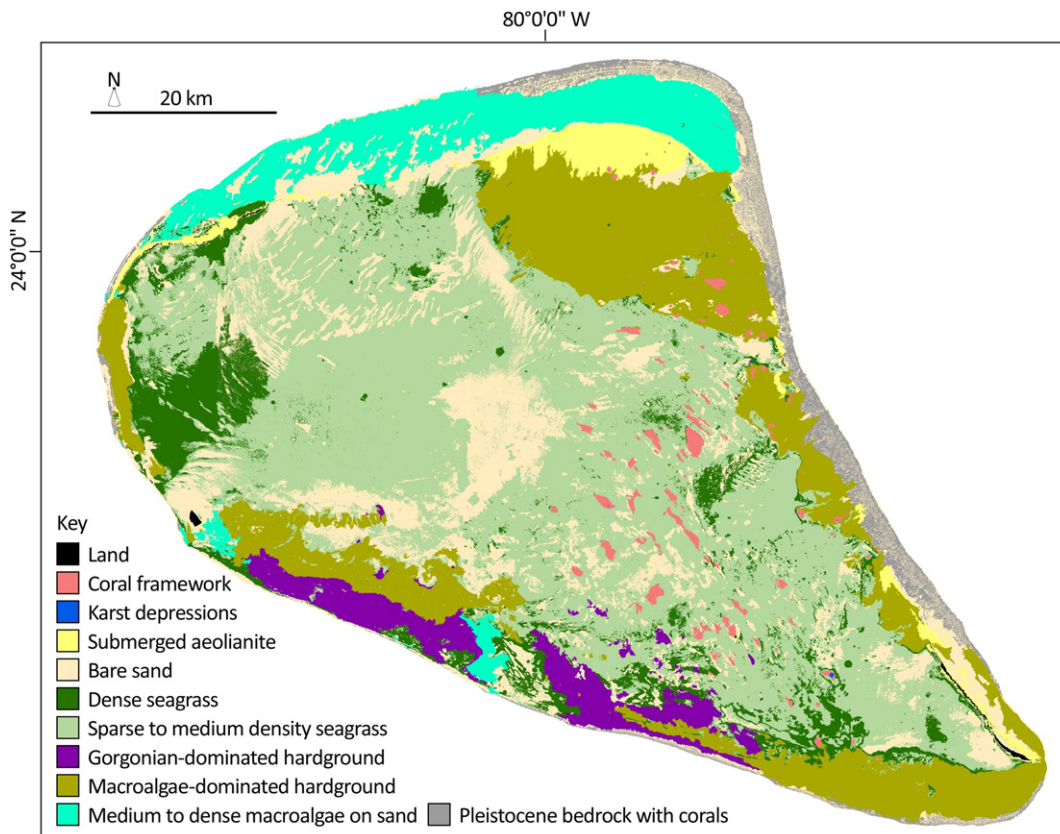


**Fig. 3.** Habitat map of Cay Sal Bank created from Worldview-2 satellite imagery and calibrated by field survey. The 11 habitat classes are described in Table 1.



penetration in tropical waters (Bosscher and Schlager, 1993; Purkis et al., 2002; Purkis and Pasterkamp, 2004). This level of penetration facilitated habitat mapping to be conducted for the entire platform-top and significant portions of the upper platform's flanks.

Segmentation of the WV2 into spectral biotopes – interpreted to be distinct bodies of uniform benthic character with common spectral properties – was achieved using a combination of edge-detection, spectral and textural analysis, and manual editing. On the basis of field observations, 11 classes (Table 1) were identified into which the spectral biotopes were assigned to generate a habitat map (Fig. 3). This map was created using the object-based image analysis software eCognition (v. 8) and assessed for accuracy against 200 ground-truth points at which seafloor video had been collected. These ground-truth points, which had not been used to guide map creation and thus could be used to quantify error, reveal the habitat map to have an overall accuracy of 85%. The majority of the inaccuracy of the map occurred between classes “macroalgae-dominated hardground” and “medium to dense macroalgae on sand”, undoubtedly due to their spectral similarity.

### 3.2. Satellite mapping of bathymetry

Following the ratio-algorithm method of Stumpf et al. (2003), approximately five million single-beam depth soundings collected in the field were used as training data to tune the algorithm's coefficients and spectral bathymetry was extracted from the WV2. A digital elevation model (DEM) was constructed for the platform-top of CSB. This DEM captures seabed topography from the low-water mark to 30 m water depth and has a spatial resolution of 2 m × 2 m, that of the WV2 imagery from which it was derived. Vertical resolution of the DEM is 0.01 m. The WV2 and field data report the majority of the platform-top of CSB to be covered by only a thin veneer of Holocene sediment. In many places, sediment is absent and the Pleistocene bedrock surface exposed. For instances when the bedrock was covered, sediment thickness was quantified by two methods. First, by examination of digital subbottom profiles, and second, by measurements made on SCUBA using a steel spike hammered into the seabed until reaching bedrock. With very few exceptions, both methods revealed the covering of Holocene sediment to be only a veneer of several centimeters thickness. For this reason, the satellite-derived bathymetry map is also a good representation of the depth of the Pleistocene bedrock surface

below present sea level. Average platform depth is 12 m and the Pleistocene margins of CSB lie at depths between 15 m and 30 m.

### 3.3. Satellite sea-surface temperature

Sea-surface temperature (SST) satellite data derived from the MODIS (Moderate Resolution Imaging Spectroradiometer) Aqua thermal IR channels (11–12 micron) were archived for the broader Bahamas region for the period Jan. 2002–Dec. 2011 (Level 2 daily product data, [www.oceancolor.gsfc.nasa.gov](http://www.oceancolor.gsfc.nasa.gov); website accessed June 1st 2012). These data are acquired daily and have a resolution of 1 km × 1 km. For the purpose of our analysis we consider monthly averaged composites for the major Bahamian carbonate platforms; LBB, GBB, CSB, Cat Island platform, Hogsty, and Great and Little Inagua. Of these six focus areas, all but the CSB and the Cat Island platform have aggraded platform margins (Hine and Steinmetz, 1984; Dominguez et al., 1988).

### 3.4. Regional hydrodynamic model

A high resolution (1/100° or ~900 m) hydrodynamic model has been developed around the Florida Keys, encompassing the Florida Straits and South Florida, based on the Hybrid Coordinate Ocean Model (HYCOM) and, therefore, abbreviated as FKeyS-HYCOM (Kourafalou and Kang, 2012). The model includes all South Florida coastal and shelf areas and extends across the Florida Straits to Cuba and the Bahamas. The domain, which encompasses the CSB and surrounding waters, is chosen to ensure the proper representations of the complex South Florida coastal system, and accommodate the influence of the strong Loop Current/Florida Current (LC/FC) system and associated eddies. The FKeyS-HYCOM is embedded in a hierarchy of larger scale models (Gulf of Mexico to North Atlantic Ocean). Therefore, it receives the appropriate variability of the large-scale regional currents, which are dominated by the LC/FC system, an integral part of the Gulf Stream. HYCOM is a comprehensive, three-dimensional hydrodynamic model with data assimilative capabilities, advanced mixing schemes and a hybrid vertical coordinate system that is flexible in isopycnal, z-level and sigma discretizations. The community available code and details on model attributes are given at <http://hycom.org>. Simulations with FKeyS-HYCOM were used to provide insight into the hydrodynamics of CSB.

**Table 1**  
Descriptions of the 11 habitat classes.

Habitat class	Description
Land	Emergent aeolianite cays and ridges
Coral framework	Areas with coral framework (e.g., <i>Montastraea</i> spp., <i>Porites</i> spp., <i>Agaricia</i> spp.) shallower than 10 m water depth and located in the platform-interior. The class commonly occurs in a leeward association with under- and in-filled karst depressions. Live coral cover <15%
Karst depressions	Karstic depressions with throats >10 m in width. When under-filled with sediment, walls are near vertical. Halimeda often abundant in throat. If depression is in-filled with sediment, dense seagrass meadows may colonize areas atop the buried depression
Submerged aeolianite	Tops of submerged aeolianite ridges colonized by a veneer of turf algae with sparse (<5%) invertebrate cover (scleractinians, gorgonians, poriferans). This class occurs when emergent aeolianite deposits are inundated to form submarine ridges. The ridges mirror platform geometry, run parallel, and in close proximity, to the platform-margin
Bare sand	Unconsolidated rippled sand sheets with little to no growth of invertebrates, seagrasses, or macroalgae. The category occurs at all depths
Dense seagrass	Sand inhabited by dense (>60% cover) seagrass meadows dominated by <i>Thalassia testudinum</i> . Other seagrasses (e.g., <i>Syringodium filiforme</i> ) and macroalgae may be admixed, but at low density. The class is found in the platform-interior and increases in abundance towards the west of the CSB. Occurrence is between water depths of 2 m and 15 m
Sparse to medium density seagrass	Sand with <60% seagrass cover. Dominant species are <i>Thalassia testudinum</i> and <i>Syringodium filiforme</i> . This class is most abundant in the platform-interior between water depths of 3 m and 15 m
Gorgonian-dominated hardground	Low rugosity sandy hardgrounds inhabited by dense gorgonian stands (>10 individuals per sq. m). Abundance increases towards the south of the CSB, between water depths of 2 m and 10 m
Macroalgae-dominated hardground	Low rugosity, rubble-dominated hardground inhabited by macro- and turf-algae with sparse (<5%) invertebrate cover (e.g., scleractinians, gorgonians, poriferans). This class is encountered in proximity to the platform-margins in water depths ranging from 5 m to 25 m
Medium to dense macroalgae on sand	Unconsolidated sand with <5% seagrass cover and relatively high (>60%) macroalgae cover. Located adjacent to the platform-margin and leeward of the reef crest in water depths >5 m. Macroalgae are typically calcareous
Pleistocene bedrock with corals	Pleistocene bedrock without sediment cover sparsely colonized by isolated scleractinian coral colonies ( <i>Montastraea</i> spp., <i>Diploria</i> spp., <i>Dendrogyra cylindrus</i> ), gorgonians, poriferans, and macroalgae. The class is associated with the platform-margin and in plan-view adopts spur-and-groove geometries orientated normal to the margin. The depressions (grooves) are sand filled. Live coral on the spurs is <20%. The class is restricted to waters depths >10 m.

### 3.5. Quantifying the lateral extent of the Bahamas carbonate platforms

Landsat ETM+ images were assembled to cover the extent of the CSB, LBB, and GBB. From these images, a “width map” was generated which uses color to describe the minimum distance from any point atop each carbonate platform to the periphery of that platform (Fig. 4). This step was accomplished by creating a mosaic of the Bahamas from the Landsat data and reducing it to a binary representation where image pixels corresponding to platform-tops were assigned a value of ‘1’, and everything else as ‘0’. A Euclidean distance transform was then computed on the binary image which assigns a number to each pixel that is the distance between that pixel and the nearest nonzero pixel. This number is equivalent to the minimum distance to the platform-margin. The purpose of generating the width map is to highlight differences in the lateral extent of the Bahamas carbonate platforms.

## 4. Results

### 4.1. Satellite mapping of habitats and bathymetry

The satellite-derived habitat map of the CSB shows the platform-interior to be sandy, with vast meadows of sparse to medium density seagrass (Fig. 3, class descriptions in Table 1). Platform-top coral frameworks are confined to the eastern-half of the platform and are small in size (<500 m diameter). Hardgrounds, dominated by gorgonians and macroalgae, become more prevalent as the platform-margin is approached. Karst depressions are frequent atop the platform and attain widths of many hundred of meters. Space cover by live corals on the platform margins is <20%.

Field observation showed the emergent cays on the platform-top to be built from a semi-continuous aeolianite ridge that rims the north and east platform-margins. The ridge can be traced between the numerous emergent cays as a narrow marine topographic high with several

meters of vertical relief and width of ~100 m. The Cat Island platform, a windward promontory of the GBB, is similarly rimmed by an aeolianite ridge (Dominguez et al., 1988). Studies from Cat Island and elsewhere in the Bahamas report such aeolianites that are exposed at, or above, present sea level as younger than 500,000 yrs BP (Carew and Mylroie, 1995), with episodes of deposition during sea-level highstands stretching into the Holocene (Halley and Harris, 1979; Kindler and Mazzolini, 2001).

### 4.2. Sea-surface temperature

MODIS-Aqua SST satellite data were archived for six focus areas, four with aggraded margins (LBB, GBB, Hogsty, and the Inaguas) and two with non-aggraded margins (CSB and the Cat Island platform). This division was made to search for systematic differences in ocean climate for the platforms with aggraded vs. non-aggraded platform-margins. The objective is to examine whether ocean climate may be a relevant factor to the depauperate development of CSB platform-margin coral reefs. Daily SST data acquired for the period January 2002–December 2011 were averaged to monthly composites and graphed (Fig. 5). Clear trends are evident in the dataset. The two largest Bahamas platforms, LBB and GBB, have markedly cooler winter water temperatures than the smaller platforms. The two smallest platforms, Hogsty and the Inaguas, are 4° to 5° warmer in the winter than LBB and GBB, but up to 2° cooler in the summer. Importantly, the two platforms with non-aggraded margins (CSB and the Cat Island platform) show no differences in sea temperature to the four platforms with aggraded margins.

### 4.3. Hydrodynamic modeling

FKeyS-HYCOM was used to compute monthly averaged near-surface currents for the years 2004–2010 for the CSB and surrounding waters.

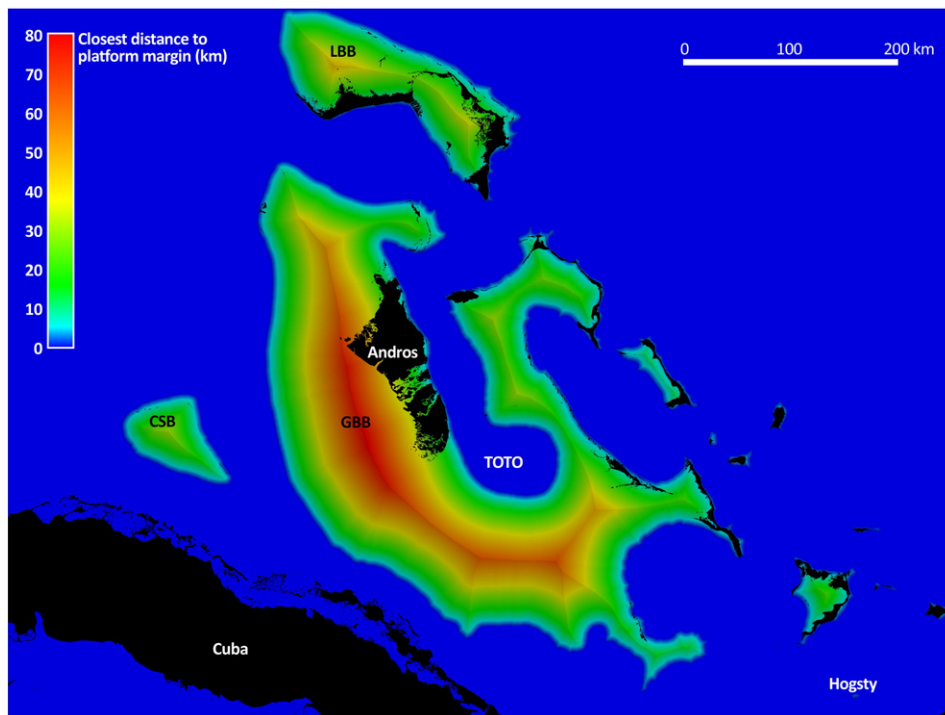


**Fig. 4.** Planform width map of the Bahamas carbonate platforms. Hotter colors demark wider, more laterally expansive, platforms. For instance, the central axis of the Great Bahama Bank (GBB) is offset from the bank's margin by 80 km. The central axis of the Little Bahama Bank (LBB) and Cay Sal Bank (CSB), by contrast, are offset by half that distance. TOTO = Tongue of the Ocean. Landmasses are colored black and deep water is colored blue.

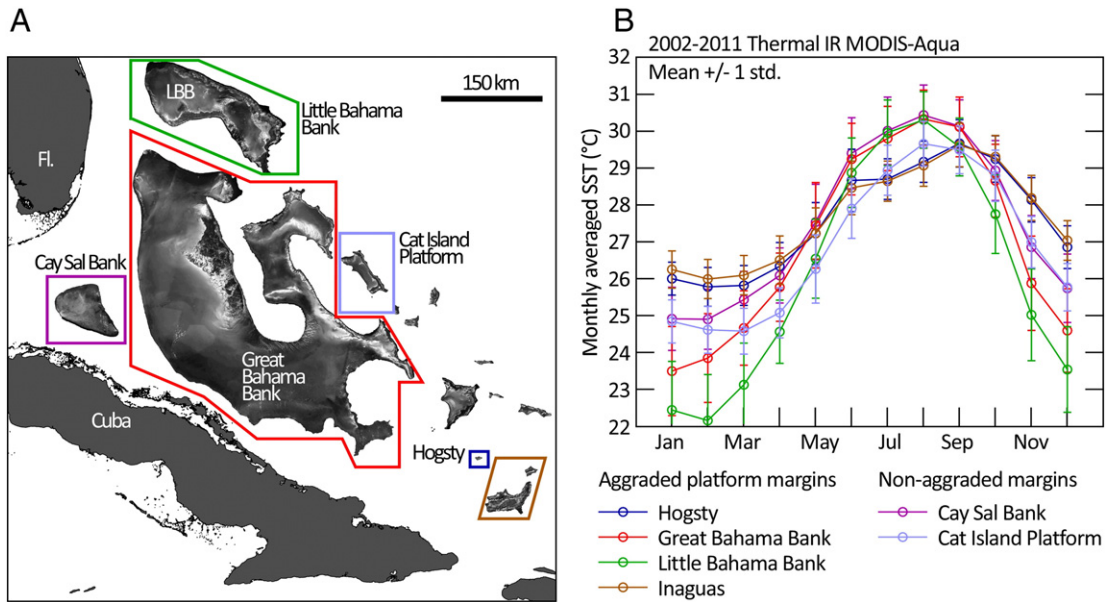


**Fig. 5.** A) The six focus areas for which MODIS-Aqua sea-surface temperature (SST) data were assembled. B) Plot of mean monthly SST for the six focus areas (circles)  $\pm$  1 standard deviation (error bars) for the period Jan. 2002–Dec. 2011. The largest platforms (Great and Little Bahama Bank) display cooler winter temperatures than the smaller platforms. Hogsty and the Inaguas, both small platforms, report warmer winters and cooler summers than the large systems. The platforms with non-aggraded margins (CSB and Cat Island platform) show no difference in ocean climate to those with aggraded margins.

Though the model revealed some inter-annual variability, it was minor and the annually averaged results were sufficient to demonstrate the salient trends. The FKeyS-HYCOM output for 2010 was representative (Fig. 6A). Here, the northeastward to northward flow of the Florida Current (FC), a branch of the Gulf Stream, dominates the hydrodynamics of the area, but remains confined to the deep topography of the Florida Straits and does not incur onto the platform-top of CSB. Annually

averaged near-surface current flow across the platform-top of CSB is at a rate of only 0.1 m/s, an order of magnitude slower than the adjacent FC, and in an east–west (westward) direction, suggesting influence of trade winds (easterlies) that dominate this region (Fig. 6B).

#### 4.4. Sediment distributions

The grain-size map interpolated from 90 surficial sediment samples reveals trends in sediments distribution (Fig. 7) which are supported by differences in statistical parameters of grain-size calculated following Folk and Ward (1957) (Fig. 8). Mud is absent atop CSB. As reported for other incipiently drowned platforms, such as the Pedro and Serranilla banks (Glaser and Droxler, 1991; Triffleman et al., 1992), mud is likely winnowed off-shelf by strong platform-top hydrodynamics. High-resolution model results from FKeyS-HYCOM do not indicate the FC to influence the platform-top. Instead, an east-to-west current is driven by the easterly trade winds, sustaining a gradient that is reflected in the distribution of sediments. The CSB can be divided into two broad precincts based on grain-size. A northeastern precinct covers approximately half of the platform-top and is characterized by sand-sized sediments (0.06 mm–2 mm, 4 to  $-1$  phi), a grainstone in the Dunham classification. By comparison, a southwestern precinct is composed of grains with up to 50% contribution by gravel ( $>2$  mm,  $<-1$  phi), a rudstone.

The northeastern and southwestern precincts show differences in mean grain-size and sorting. On the basis of the statistical parameters of Folk and Ward (1957), the stations in the northeastern precinct span very poorly sorted to moderately sorted, as compared to those in the southwestern precinct which are less diverse and only range from poorly to moderately sorted (Fig. 8). The two precincts can also be differentiated on the basis of mean grain-size, though some overlap exists because of the occurrence of pockets of medium sands in the northeastern precinct associated with the Muertos, Damas and Anguilla Cays, and the Dog Rocks (Fig. 7). While the majority of the stations in the northeastern precinct have a mean grain-size equating to coarse sand and gravel, as classified by Folk and Ward (1957), there are several instances where medium sands were sampled platformward of aeolianite cays in areas dominated by seagrass.

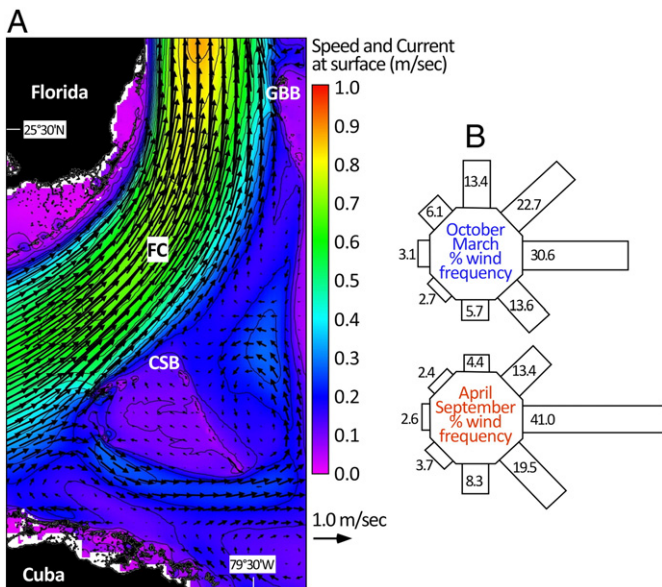


**Fig. 6.** A) 2010 annually averaged surface currents (vectors and color for speed) for the Cay Sal Bank (CSB) and surrounding waters computed with the Florida Straits, South Florida and Florida Keys Hybrid Coordinate Ocean Model (FKeyS-HYCOM). The Florida Current (FC) does not incur onto the platform top of the CSB. B) Seasonally averaged winds for the CSB for the year 1975 (upper, dry season: October–March; lower, wet season: April–September). U.S. Naval Weather Service Command – modified from Goldberg (1983). The CSB sits in the trade wind belt and winds are principally from the east during most of the year, with secondary peaks from the northeast during the dry season and from the southeast during the wet season.



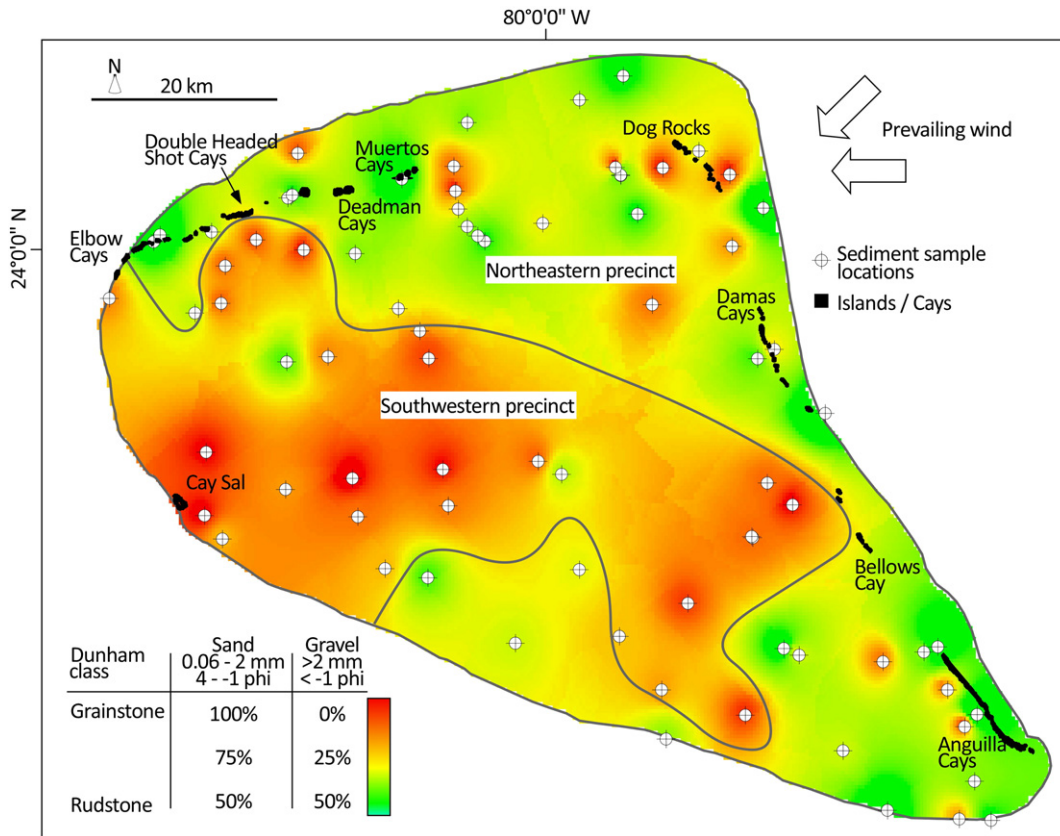


**Fig. 7.** Grain-size distribution map for Cay Sal Bank interpolated from 90 surficial sediment samples. The platform-top can be partitioned into two precincts on the basis of grain-size. The northeastern precinct is more grainy than the southwestern, a gradient consistent with influence of prevailing trade winds.

**5. Discussion**

Subbottom profiles run normal to the platform-margin of CSB indicate sands which have accumulated on the southern and western flanks to have a maximum thickness of 20 m and thin platformward. Sediment accumulation on the flanks is in stark contrast to the platform-top which is largely devoid of sediment. The acoustic reflector corresponding to Pleistocene bedrock, which can be traced from the platform-top,

beneath the bank-edge sand body and down the flanks of CSB, shows no evidence of Holocene reefs (Fig. 9).

While the easterly trade winds are interpreted to control the distribution of sediments atop CSB, (Fig. 7), there is evidence that the FC influences the deep (>200 m) flanks of the platform. This influence can also be inferred through inspection of the subbottom data. Profiles acquired across the western flank of CSB report a 40° slope angle which persists from the shelf-break down to 300 m water depth, the profile's

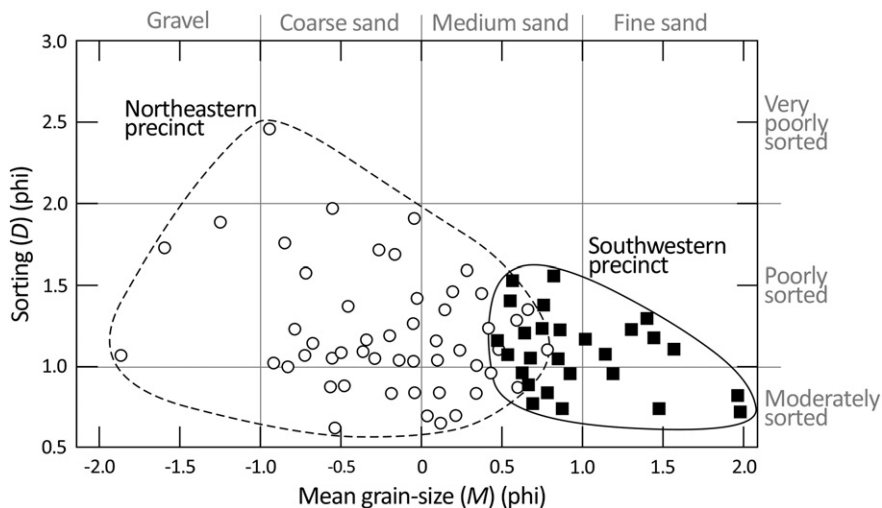


**Fig. 8.** Scatterplot of mean grain-size (M) versus sorting (D) calculated following Folk and Ward (1957) for 90 surficial sediment samples. Differences in these statistical parameters support the partitioning of the Cay Sal Bank into two precincts.

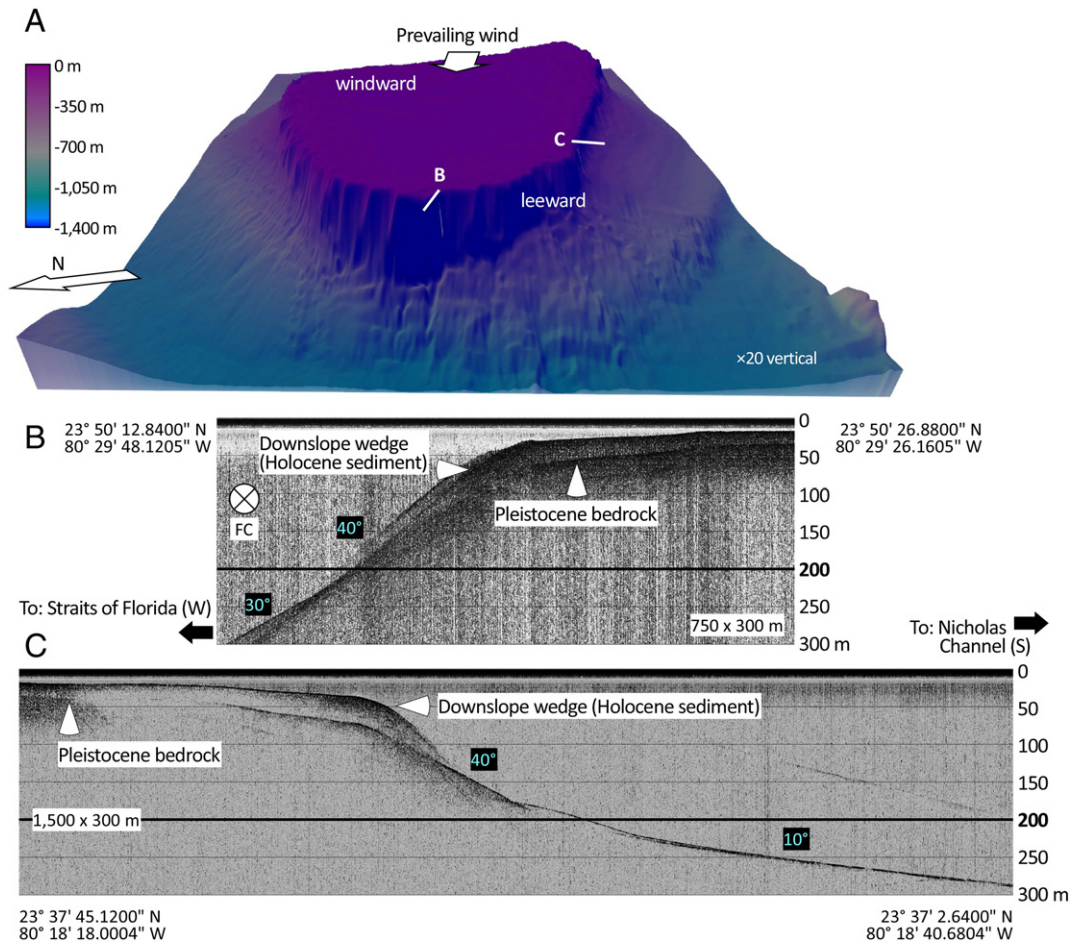


**Fig. 9.** A) Seafloor morphology of Cay Sal Bank based on National Ocean Service Hydrographic Survey Data showing the position of two down-flank subbottom profiles, 'B' normal to the bank's western margin, and 'C' normal to the southern margin. Prevailing wind is from the east. B) Subbottom profile across the western flank of the platform shows approximately 20 m thickness of Holocene sediment overlaying featureless Pleistocene bedrock in the form of a downslope sediment wedge. There is no indication for up-growth of Holocene reefs from the Pleistocene surface. The declination angle for the flank is 40° down to 200 m below present sea level, flattening to 30° from 200 m to 300 m depth. C) Subbottom profile across the southern flank of the platform. As for 'B', the Pleistocene bedrock is featureless and the development of platform-margin reefs is not evidenced. Like 'B', the flank's declination for 'C' is 40° down to 200 m below present sea level, but flattening to only 10° at greater depth. We interpret the difference in declination of the slope beyond 200 m between 'B' and 'C' to be related to the Florida Current (FC) which interacts only with CSB's western margin.

end (Fig. 9B). By contrast, an equivalent profile across the southern flank shows the same declination down to a depth of 200 m, beyond which the angle reduces to 10°. The reduced slope angle is caused by an extensive sediment wedge which, on the basis of Hine and Steinmetz (1984), is interpreted to be an accumulation of periplatform sands (Fig. 9C). Differences in flank geometry can be explained by the influence of the FC. We interpret the current to strongly interact with the western margin of the platform (Fig. 6A), incising the deep flank, excavating the periplatform sediment wedge, and hence, steepening the flank's angle of repose.

Seafloor morphology of CSB, based on National Ocean Service Hydrographic Survey Data, shows the presence of a sediment wedge below 200 m water depth on the northern and southern margin of CSB, a feature absent from the west (Fig. 9A). Hine and Steinmetz (1984) report the periplatform sediments to contain *Halimeda*, molluscs, and non-skeletal components derived from shallow water. On the basis of the subbottom profiles, it is suggested that the FC remains confined to the deep topography of the Florida Straits, exerting direct influence only on the western flank of CSB at water depths exceeding 200 m. This is an important observation. Triffleman et al. (1992) hypothesized that incursions of the FC atop the CSB may serve to explain its inability to retain platform-top sediments and accrete at a sufficient rate to track rising Holocene sea-level. Inspection of flank profiles and

results from the FKeyS-HYCOM would indicate the FC to have little to no influence on the platform-top.

### 5.1. Why does the Cay Sal bank lack platform-margin coral reefs?

There are several detached platforms in the Caribbean where carbonate accretion is failing to keep pace with Holocene sea-level rise. Serranilla Bank (1100 sq. km in area) which is located on the Nicaraguan Rise, like CSB, lacks the extensive development of platform-top reefs and is barren of sediment (Triffleman et al., 1992). Serranilla also lacks windward and leeward platform-margin coral reefs and is only framed by non-aggraded margins that languish in water depths of 30 m–40 m, well below the 10 m limit of maximum carbonate production (Schlager, 1981). Similarly sized to Serranilla Bank, the Cat Island platform covers an area of 1500 sq. km and is afforded no protection by its 20 m–30 m deep non-aggraded margins (Dominguez et al., 1988). The CSB is analogous to both Serranilla Bank and the Cat Island platform in terms of its deep platform-top and margins. Lacking "keep-up" margin reefs, the bank-top environments of all three sites are exposed to substantial wave and current energy, akin to open marine conditions, which serve to export any produced sediment off-platform; export-dominated systems as defined by Kleypas et al. (2001). Sediment loss condemns the platforms to be outpaced by sea-



level rise. While for now still within the photic zone, the platforms are in the process of drowning as carbonate loss outweighs carbonate production. This morphology is in stark contrast to the adjacent GBB – a platform accreting at a sufficient pace to remain within the 10 m zone of maximum carbonate production. Accretion is enabled by shallow, active “keep-up” coral reef margins that serve to both produce sediment and prevent its loss into deep water.

In comparison to Serranilla Bank and the Cat Island platform, CSB is conspicuous in its large size (6000 sq. km). Grigg and Epp (1989) noted that the depth of drowned Holocene banks is often negatively correlated with summit area; smaller banks are typically deeper. Hine and Steinmetz (1984) suggested that the efficiency of sediment removal is inversely related to bank size; the smaller the bank, the shorter the distance from any point on the bank-top to the deep sea. If a true relationship, the width maps for the Bahamas platforms (Fig. 4) also portray efficiency of sediment loss. In the framework of Grigg and Epp (1989), CSB can therefore be considered as an outlier; it is very large but also unable to keep pace with Holocene sea-level rise. It is fair to ask why the vast CSB is so different from its neighbors. The deep platform-top is at least partially drowned, or perhaps even in the early stages of complete drowning.

### 5.2. Inimical waters?

One explanation forwarded to explain the lack of platform-edge reefs on carbonate platforms is the “inimical bank water” effect (Schlager, 1981). This is the tendency for shallow bank-top waters to equilibrate rapidly with the atmosphere relative to the more deeply mixed oceanic waters that front the platform-edge reefs (Neumann and Macintyre, 1985). Bank-top waters are rendered inimical by extreme cooling during the passage of winter cold fronts. Flushing of the chilled water over platform-margin reefs serves to retard their development. Ginsburg and Shinn (1964) noted that the major reefs of south Florida occur seaward of Pleistocene limestone islands and attributed the scarcity of thriving reefs opposite the large tidal passes of the Florida Keys to be related to inimical waters moving through the passes. The

flushing of plumes as cold as 16 °C have been captured by satellite for the middle Florida Keys (Roberts et al., 1982, 1992), with reports of a 1977 cold front depressing water temperatures as low as 9 °C (Hudson, 1981).

The inimical bank water effect has also been considered in the context of the GBB (Newell et al., 1959) and evoked to explain the 3 kyr and 4 kyr BP demise of the *Acropora*-dominated reefs of the Florida shelf (Lighty et al., 1978; Ginsburg and Shinn, 1994) and LBB (Lighty et al., 1980). Neumann and Macintyre (1985) described these reefs to have been “shot in the back by their own lagoons”. Winter cooling can be imaged by SST satellites. For instance, a MODIS-Aqua SST image captured in February 2010, reports patterns in sea temperature consistent with the formation of inimical waters (Fig. 10). While the surface of the Florida Straits and Nicholas Channel have temperatures exceeding 25.5 °C, the platform-top waters of GBB and LBB are depressed by several degrees. The image also reports an area of cool water in the center of CSB and similarly over the Florida Keys island chain and Reef Tract. Such preferential cooling of shallow areas is typical of winter patterns in coastal and shelf seas and particularly pronounced in tropical environments, surrounded by much warmer open sea waters. We are cognizant that this image represents a snapshot in time and while it cannot be used to infer SST patterns on Holocene, annual, or inter-annual time-scales, the data are valuable in demonstrating the potential for winter cooling of platform-top waters.

There exists a contradiction, however, in the application of the inimical bank water effect to explain the depauperate shelf margin of CSB. The maximum distance from the platform-interior to the margin of CSB, 40 km, is half of that for GBB (80 km) (Fig. 4). Because of the larger area of shallow water, it can be assumed that the much greater breadth of the GBB would render it considerably more susceptible to the development of cold inimical waters, as compared to CSB. Counter to this observation, the leeward margin of the GBB hosts prominent bank-edge reefs (Hine and Steinmetz, 1984), whilst CSB, situated just 50 km to the west across the Santaren Channel, lacks them (Fig. 9). The evidence for the stunting of platform-margin reefs by inimical waters is therefore weak.

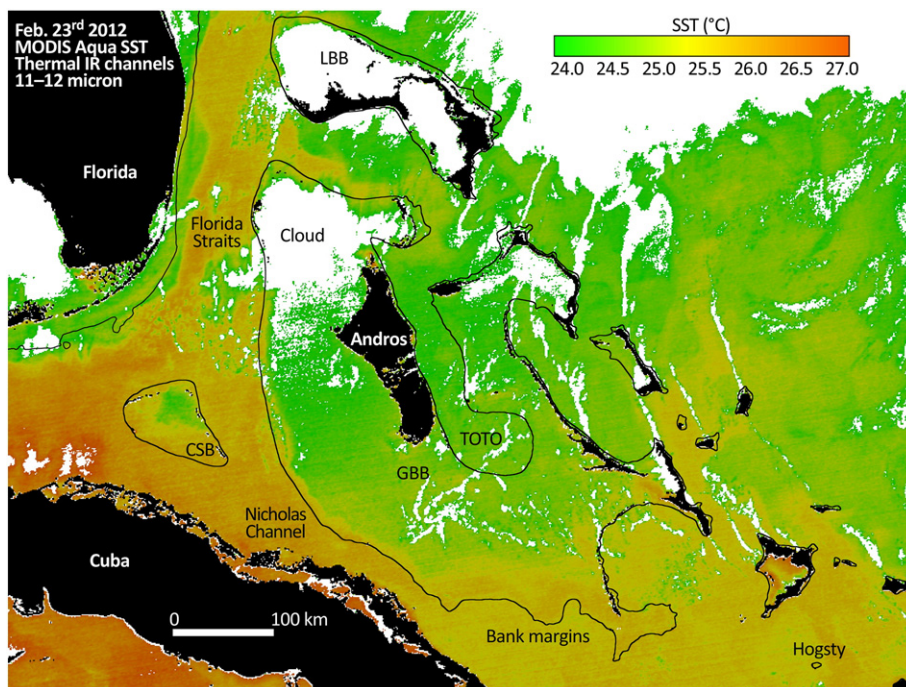


**Fig. 10.** Sea-surface temperature (SST) satellite data for the Bahamas, acquired February 23<sup>rd</sup> 2010. These data have a 1 km × 1 km resolution and are derived from the MODIS-Aqua thermal IR channels. White areas are cloud contaminated and contain no data. The pattern of SST shows the cooling of waters atop the Great Bahama Bank (GBB) and Little Bahama Bank (LBB), the outflow from which has cooled the Tongue of the Ocean (TOTO). Similar cooling of surface waters, but to a lesser extent, can be seen atop Cay Sal Bank (CSB).

### 5.3. Ocean climate?

Beyond inimical winter waters, regional-scale variations in ocean temperature are sufficient to alter growth potential in the dominant species of Caribbean zooanthellate corals (Houck et al., 1977; Hubbard and Scaturro, 1985), an effect that can deliver differences in aggradation between carbonate platforms over Holocene timescales (Dullo, 2005). For example, present-day latitudinal limits of reef growth can be explained by the decrease in reef-coral diversity which falls in a marked and tight regression with decreasing water temperatures along north-south coast lines such as Japan, Australia, or Florida (Veron and Minchin, 1992; Veron, 1995).

A decade of daily MODIS SST records was assembled for the Caribbean (Fig. 5) to investigate the relevance of temperature variation on the lack of margin-reef development on CSB, versus the reef-rimmed platforms of nearby GBB, and most drastically, the fully aggraded margins of Hogsty reef atoll located 660 km to the southeast (Pierson and Shinn, 1985). It is well established that elevated sea temperatures cause widespread coral bleaching and mortality (Glynn, 1993; Brown, 1997; Hoegh-Guldberg, 1999; Berkelmans, 2002), as equally can low temperatures (Hoegh-Guldberg et al., 2005), particularly so in the Caribbean (Kemp et al., 2011). The decade of MODIS SST does report pronounced seasonality. However, the data do not evidence differences in seasonal maximum or minimum temperature between the Bahamas platforms with aggraded margins (GBB, LBB, Inaguas, and Hogsty) and non-aggraded margins (CSB and the Cat Island platform) (Fig. 5).

We recognize that the decade-long time series is insufficient to infer regional temperature trends for the Holocene Caribbean, though two observations suggest ocean temperature to be unrelated to the regional development, or not, of “keep-up” platform-margin reefs. First, while CSB lacks an aggraded margin, seismic data from the western (leeward) GBB show 12–15 m high margin reefs buried beneath thick sand deposits (Hine and Steinmetz, 1984). The maximum distance between the two platforms of 60 km can be presumed too little for the expression of any regional differences in ocean temperature. Second, studies of Caribbean paleoclimate variability during the Holocene indicate a regional and progressive transition from cool and dry to warm and wet conditions (Peterson et al., 1991; Hodell et al., 1995; Kerwin et al., 1999), unaccompanied by hiatus in reef development. On the balance of these observations, the influence of ocean climate on the absence of reef growth on CSB is weak.

### 5.4. Hydrodynamics?

Based on flume experiments and theoretical considerations, high water movement may impede settlement of coral larvae and play a major role in determining the spatial distribution of corals atop platforms characterized by high rates of flow (Abelson, 1997). Located in the central Florida Straits, CSB is an obstacle to the northerly passage of the FC and causes a diversion of flow to the south of the bank into the Nicholas and Santaren channels (Leaman et al., 1995; Hamilton et al., 2005; see also Fig. 6).

Fast water movement over rough substratum induces accelerating laminar, thin boundary-layer flows uncondusive to the settlement of larvae, even if chemical and other cues are favorable (Abelson et al., 1994). The hypothesis proposed here is that the FC exerts a hydrodynamic impediment to reef development atop CSB. If true, this would offer a plausible explanation for the immature platform-top processes which stand in stark contrast to the shallower, more active, GBB. The latter platform is uninfluenced by the FC. To test this hypothesis, we examine regional-scale runs of FKeyS-HYCOM in combination with our own sedimentologic observations.

Yearly averaged numeric simulations from 2010 using FKeyS-HYCOM indicate that the platform-top of CSB is uninfluenced by the FC (Fig. 6). Instead, the current is confined to the deep topography of the Florida Straits, likely obeying vorticity constraints. Being a yearly

average, the simulations lacks the eddy influence discussed by Kourafalou and Kang (2012), but even on short timescales, model runs do not indicate sustained incursion of the FC onto the platform-top of CSB. Goldberg (1983) reports winds for the CSB to be principally from the east during most of the year (trade winds), shifting to the northeast during winter. This corroborates the FKeyS-HYCOM annually averaged outputs that show a weak (<0.1 m/s) easterly current across the platform-top (Fig. 6). The model predictions are similar to the reported hydrodynamics of GBB (Smith, 1995; Roth and Reijmer, 2004).

Further insight into the hydrodynamic gradient atop CSB can be gained from the platform's sedimentology and, in particular, the infill pattern of sinkholes, locally termed “blue holes”. Detailed mapping from WV2 satellite imagery, calibrated by field survey, shows the seafloor of CSB to be riddled with visible and buried karst topography. The diameters of karst depressions range from 30 m to 500 m (Fig. 3). It is apparent that the majority of sinkholes are filled with sediment. However, as reported by Dodd and Siemers (1971) for the Florida Keys, this karst topography, developed during the lowered sea level of the Pleistocene, strongly controls Holocene sediment thickness and present biotic distribution. It is for this reason that buried sinkholes on CSB can be recognized through examination of the contemporary patterning of seagrass meadows and platform-top patch reefs.

We investigated the geometry of numerous active and buried sinkholes using subbottom profiles. These data reveal asymmetric infill of sediment into unfilled sinkholes. Asymmetric patterns of infill provide insight into the direction of sediment transport. A better developed sediment wedge is routinely found against the eastern (windward) wall of the depression than the western (leeward) wall, indicating an east-west transport of sediment across the platform-top (Fig. 11A). This infill pattern corroborates the direction of water movement reported by FKeyS-HYCOM and reinforces the assertion that easterly trade winds exert principle control over CSB's platform-top hydrodynamics.

Subbottom profiles acquired over buried sinkholes reveal a circular meadow of dense *Thalassia testudinum* seagrass to be diagnostic of an underlying karst depression (Fig. 11B). Though we lack data to support the hypothesis – it was not central to our study – the association between seagrass and sinkholes can likely be explained by the liberation of nutrients as the infilling sediment in the depressions becomes anoxic, or from the passage of anoxic groundwater through the platform's karst system (Bottrell et al., 1991; Stoessell et al., 1993; Bennett et al., 2000; Schmitter-Soto et al., 2002). We propose that the seagrass meadows remain confined to the throats of the buried sinkholes as the outlying sediments are nutrient limited (Cate, 2009).

Platform-top reefs, like seagrass, also associate with sinkholes (Fig. 11AB). Inspection of WV2 imagery shows coral reefs to preferentially develop on the leeward (western) side of sinkholes. This association is best explained by sinkholes acting as a trap to the east-west transport of sediment across the platform. A crescentic zone of reduced sediment stress develops in the lee of the sinkhole which elongates downstream. This zone provides suitable habitat for the development of platform-top reefs which would otherwise be disadvantaged by sand sheets that drift unencumbered, because CSB lacks a sheltering reef rim, across the platform-top. Growth is impeded by sediment that settles on the coral surface (Rogers, 1990; Weber et al., 2006). This factor clearly favors the leeward edge of sinkholes as a locus of reef development. When a sinkhole is fully infilled, for the aforementioned reasons pertaining to nutrient availability, seagrass meadows will develop in the buried throat, which in turn, act as a baffle to water flow, capture sediment, and serve to maintain the leeward zone of reduced sediment stress. This hypothesis is supported by the observation that platform-top reefs on the CSB continue to associate with filled sinkholes which have been colonized by seagrass.

The important observation in the context of this study is that associations between karst topography and present biota are arranged along an east-west gradient, as would be expected under influence of the easterly trade winds. The satellite imagery does not provide evidence



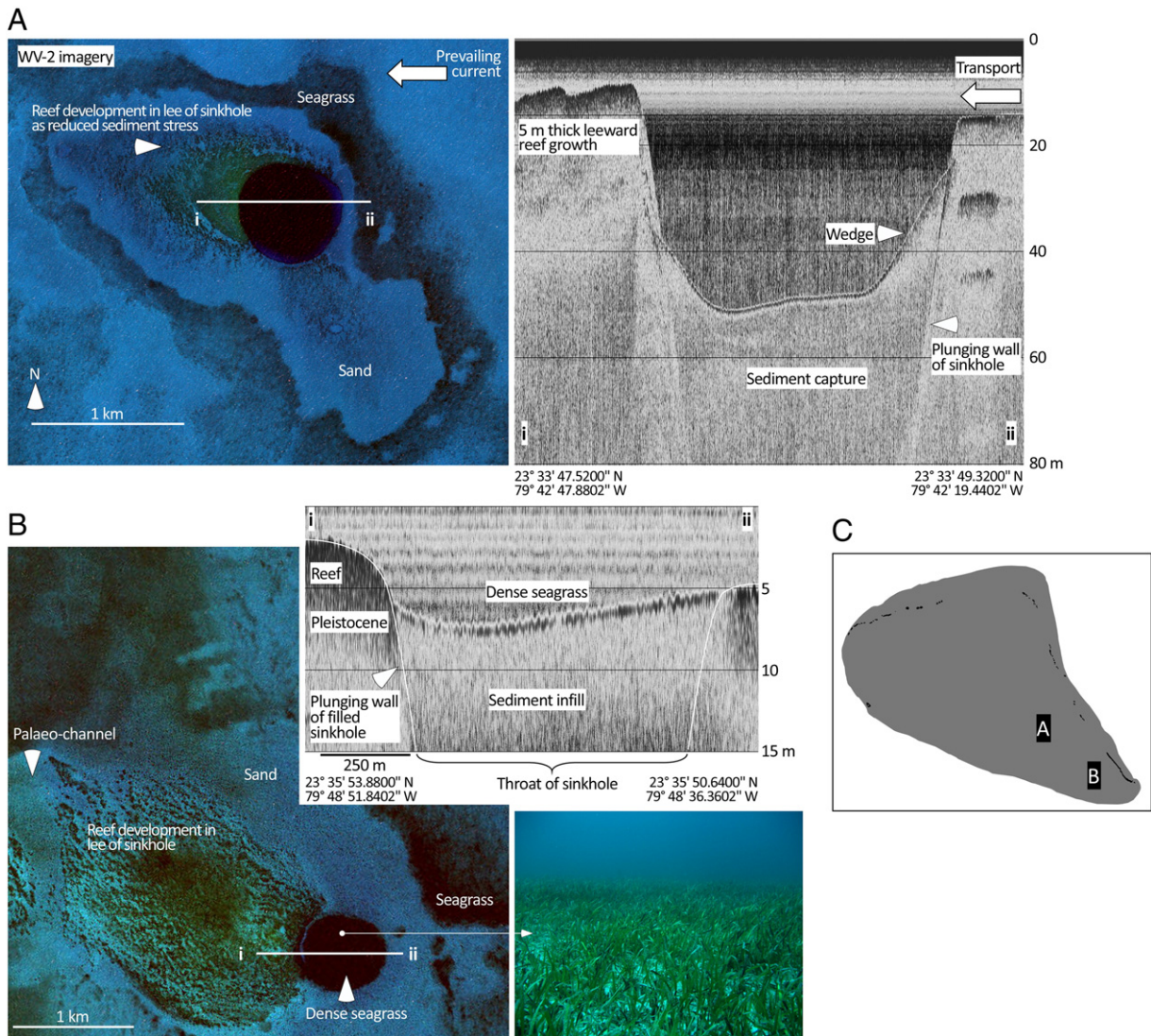


**Fig. 11.** A) Worldview-2 satellite imagery showing the placement of a subbottom profile across an unfilled karst depression (blue hole). Sediment infill is asymmetric. The sediment wedge is more substantial on the eastern (upwind) margin of the sinkhole than the western. B) A similar profile to 'A', but this profile bisects a sinkhole that has been completely infilled by sediment. The buried throat of the depression is colonized by a dense meadow of seagrass. C) Location of 'A' and 'B' on the platform top of the Cay Sal Bank. The sinkholes in 'A' and 'B' both have crescentic platform-top reefs associated with their western margins.

for north–south gradients as expected by an incursion of the FC across the platform-top. Our sedimentologic observations therefore support FKeyS-HYCOM which reports the FC to remain confined to the Florida Straits. By extension, it is unreasonable to implicate the influence of the FC in the depauperate development of the CSB reef rim.

**5.5. Holocene flooding history?**

The zone of maximum carbonate sediment production is at a water depth less than 10 m (Schlager, 1981). At the time of flooding, the extent of the platform shallower than this depth, and the time it remains there, is important because it controls the available area of carbonate sediment production which, in turn, dictates the amount of sediment available for seaward progradation, and importantly for CSB, platform aggradation (Palmer, 1979; Dominguez et al., 1988; Kim et al., 2012).

The timing of flooding of the CSB is important in understanding the modern sedimentologic conditions. Flooding history is reconstructed on the basis of the WV2-derived DEM and the Holocene sea-level curve of Toscano and Macintyre (2003, Fig. 5) for the Caribbean. We assume

negligible tectonic subsidence. Given that Holocene sediments only form a veneer of a few centimeters over the Pleistocene bedrock, the satellite-derived DEM can be taken as good representation of the depth of the Pleistocene bedrock surface below present sea level.

Inundation of CSB was compared to that of GBB. A flooding history for GBB was constructed using the satellite-derived DEM of Lee et al. (2010, Fig. 1c) which was cross-checked against literature bathymetry tracks and maps (Boss, 1996; Roth and Reijmer, 2004; Harris et al., 2011). This DEM for GBB is less reliable than that of CSB for a number of reasons. First, it is constructed from MERIS data which have a spatial resolution of only 300 m × 300 m (the CSB DEM is 2 m × 2 m). Second, far fewer depth soundings were used to calibrate the DEM for GBB (281) versus CSB (>5 million). Lastly, the thickness of Holocene sediment is better constrained for CSB than for GBB and its DEM more truthfully depicts the Pleistocene bedrock surface. Despite these limitations, the GBB DEM provides broad insight into the timing of inundation of the GBB platform-top. For both CSB and GBB, flooding will be quantified as the percentage of the platform flooded at three time intervals, in comparison to present-day platform area shallower than 30 m water depth.



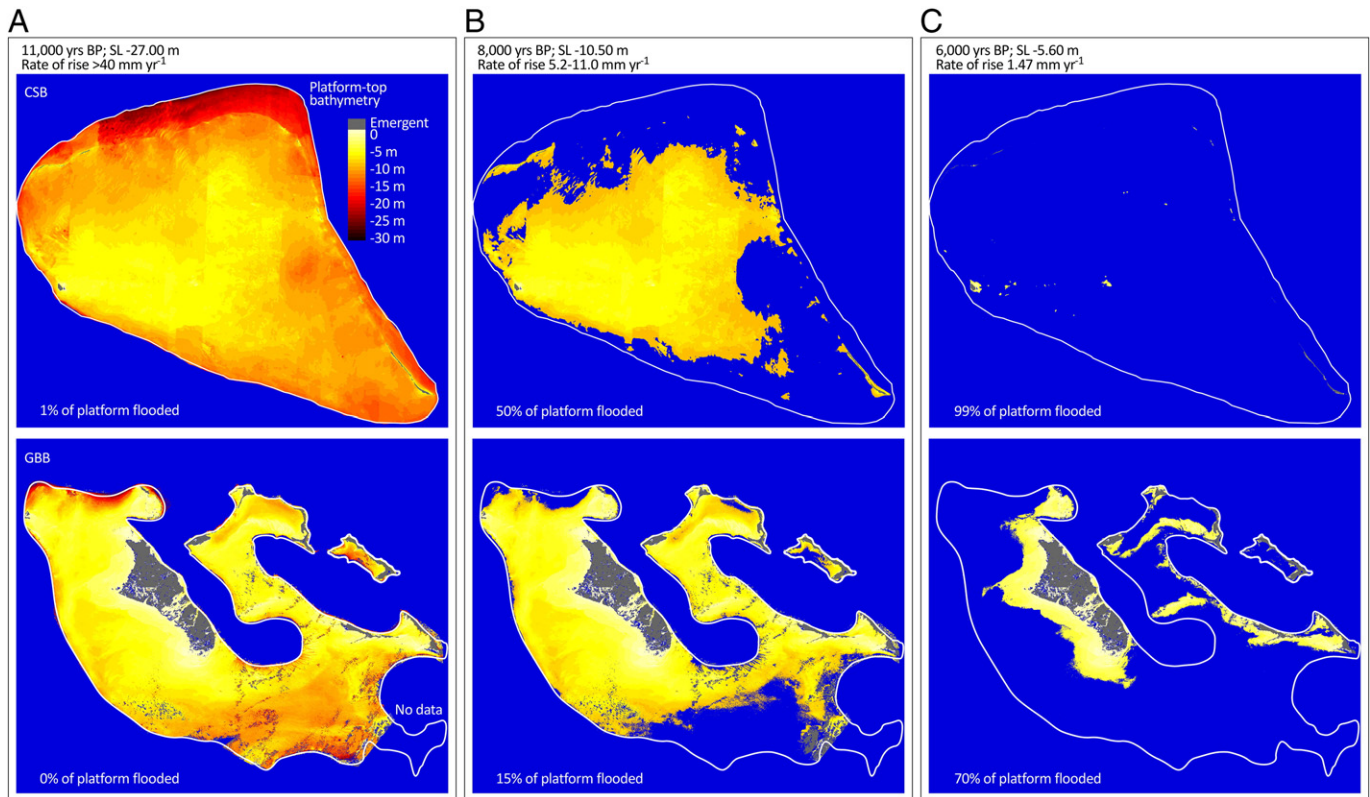


**Fig. 12.** A), B), and C) Paleogeographic maps depicting the inundation of Cay Sal Bank (CSB) (top) and Great Bahama Bank (GBB) (bottom) by Holocene sea-level (SL) rise as tracked by the curve of Toscano and Macintyre (2003). Rates of sea-level rise ( $\text{mm yr}^{-1}$ ) taken from Toscano and Macintyre (2003) from the present to 11,000 yrs BP and from Alley et al. (2005) from 11,000 yrs BP to 12,000 yrs BP. Bathymetry for CSB is WV2-derived and for GBB is from Lee et al. (2010), Fig. 1c, Z. P. Lee – personal communication (2012). Sea-level position at each time step is denoted (11,000, 8000, and 6000 yrs BP). 50% of the CSB platform-top is flooded by 8000 yrs BP at a rate 5.2–11  $\text{mm yr}^{-1}$  which equals or exceeds the “keep-up” ability of most Caribbean reefs. The platform-top of GBB is flooded later and at a slower rate.

At 11,000 yrs BP, sea level stood at  $-27$  m below present position and 1% of the CSB platform-top was inundated. The entire platform-top of GBB is emergent at this time (Fig. 12A). By 8000 yrs BP, sea level had risen to  $-10.5$  m below present position, inundating 50% of the CSB platform-top but only 15% of that of the GBB (Fig. 12B). During this time-interval, the rate of sea-level rise was between  $5.2$   $\text{mm yr}^{-1}$  and  $11$   $\text{mm yr}^{-1}$  (Toscano and Macintyre, 2003). The platform-margins of CSB flooded between 9000 yrs BP and 10,000 yrs BP at a rate of  $10$   $\text{mm yr}^{-1}$ , which is in excess of the carbonate production potential (the “keep-up” rate) of most Caribbean reefs (Neumann and Macintyre, 1985). Numeric simulations of carbonate platform evolution report that a platform can even drown during a constant relative sea-level rise whose rate is less than the keep-up rate of the platform (Kim et al., 2012). By 6000 yrs BP, sea level had risen to  $-5.6$  m below present level and 99% of the CSB platform-top was inundated. By comparison, only 70% of GBB was inundated at this time (Fig. 12C).

CSB flooded earlier and at relatively higher rates of Holocene sea-level rise than its neighboring platforms. For instance, the WV2-derived DEM reports more than 60% of the Pleistocene top of CSB to lie in water depths exceeding 10 m. By contrast, the GBB DEM reports only 20% of the GBB to lie beneath 10 m water depth. The majority of the platform-top of GBB would have flooded 1000 yrs later than CSB, after the pronounced deceleration of sea-level rise about 7.6 ka, equating to a near fourfold decrease in the rate of transgression, as measured by the sea-level curve of Toscano and Macintyre (2003). This slower rate of inundation would have better allowed depositional environments, shelf-edge coral reefs in particular, to become established and it is likely for this reason that GBB is reef-rimmed. Conversely, deeper platforms, including CSB, Serranilla Bank, Cat Island platform, and western LBB typically lack platform-margin reefs – they have “given-up”

(Wilber, 1981; Hine and Steinmetz, 1984; Dominguez et al., 1988; Triffleman et al., 1992).

## 6. Conclusion

CSB lacks an actively accreting coral-reefal rim and, for this reason, the platform-top is exposed to substantial wave and current energy which serves to export any produced sediment off the platform. Several hypotheses are investigated to explain why CSB is largely devoid of islands, lacks “keep-up” platform-margin coral reefs and holds little sediment on the platform-top, morphologies that contrast with neighboring GBB. Inspection of regional SST data report CSB to be situated in the same ocean climate regime as GBB. The Florida Current, a branch of the Gulf Stream that interacts with the CSB, but not GBB, is found to remain confined to the deep topography of the Florida Straits, approaching the western CSB margin, but without incurring onto the platform-top. This observation is corroborated by the patterns of sediment distribution atop CSB which align east-to-west and are consistent with westward platform-top currents driven by the easterly trade winds. Analysis of platform-top bathymetry shows the CSB to have flooded earlier and at relatively higher rates of Holocene sea-level rise than neighboring platforms. As is supported by numeric models (Kim et al., 2012), this study selects flooding history as key to explaining why CSB is unable to keep pace with Holocene sea-level rise.

## Acknowledgments

Financial support was provided by the National Coral Reef Institute (NCRI) and the Khaled bin Sultan Living Oceans Foundation (KSLOF). Invaluable logistical field support was provided by the crew of the M/Y

Golden Shadow, through the generosity of HRH Prince Khaled bin Sultan. Additional in country assistance was provided by the Bahamas National Trust. Dr. L. Metsamaa's work in the NCRI is supported by the Estonian Science Foundation Mobilitas postdoctoral grant. Dr. V. Kourafalou was supported by the National Science Foundation (OCE 0550732); we thank Dr. H. Kang (UM/RSMAS) for preparing the annually averaged model currents and Dr. Z. P. Lee for provision of the DEM for Great Bahama Bank. Thanks are extended to Brett Thomassie and DigitalGlobe Inc. for flexibility and unwavering assistance with acquiring Worldview-2 imagery. Landsat images came courtesy of the U.S. Geological Survey. The manuscript was improved through the insightful comments of two anonymous reviewers and Paul Kench, Editor of the Special Issue. This is NCRI contribution 152.

## References

- Abelson, A., 1997. Settlement of marine organisms in flow. *Annu. Rev. Ecol. Syst.* 28, 317–339.
- Abelson, A., Weihs, D., Loya, Y., 1994. Hydrodynamic impediments to settlement of marine propagules and adhesive-filament solutions. *Limnol. Oceanogr.* 39, 164–169.
- Alley, R., Clark, P., Huybrechts, P., Joughin, I., 2005. Ice-sheet and sea-level changes. *Science* 310, 456–460.
- Bennett, P.C., Hiebert, F.K., Rogers, J.R., 2000. Microbial control of mineral-groundwater equilibria: macroscale to microscale. *Hydrogeol. J.* 8, 47–62.
- Berkelmans, R., 2002. Time-integrated thermal bleaching thresholds of reefs and their variation on the Great Barrier Reef. *Mar. Ecol. Prog. Ser.* 229, 73–82.
- Boss, S.K., 1996. Digital shaded relief image of a carbonate platform (northern Great Bahama Bank): scenery seen and unseen. *Geology* 24, 985–988.
- Bosscher, H., Schlager, W., 1993. Accumulation rates of carbonate platforms. *J. Geol.* 101, 345–355.
- Bottrell, S.H., Smart, P.L., Whitaker, F., Raiswell, R., 1991. Geochemistry and isotope systematics of sulfur in the mixing zone of Bahamian blue holes. *Appl. Geochem.* 6, 97–103.
- Brown, B.E., 1997. Coral bleaching: causes and consequences. *Coral Reefs* 16, 129–138.
- Carew, J.L., Mylroie, J.E., 1995. Depositional model and stratigraphy for the Quaternary geology of the Bahama Islands. In: Curran, H.A., White, B. (Eds.), *Terrestrial and Shallow Marine Geology of the Bahamas and Bermuda*. Geological Society of America (Boulder CO) Special Paper, 300, pp. 5–32.
- Cate, J.R., 2009. Assessing the impact of groundwater pollution from marine caves on nearshore seagrass beds in Bermuda. (Master's Thesis) Texas A&M University, Galveston (101 pp.).
- Dodd, J.R., Siemers, C.T., 1971. Effect of Late Pleistocene karst topography on Holocene sedimentation and biota, Lower Florida Keys. *Geol. Soc. Am. Bull.* 82, 211–218.
- Dominguez, L.L., Mullins, H.T., Hine, A.C., 1988. Cat Island platform, Bahamas: an incipiently drowned Holocene carbonate shelf. *Sedimentology* 35, 805–819.
- Dullo, W.-C., 2005. Coral growth and reef growth: a brief review. *Facies* 51, 33–48.
- Folk, R.L., Ward, W.C., 1957. Brazos river bar: a study of significance of grain size parameters. *J. Sediment. Petrol.* 27, 3–26.
- Ginsburg, R.N., Shinn, E.A., 1964. Distribution of the reef-building community in Florida and the Bahamas. *Bull. Am. Assoc. Pet. Geol.* 48, 527.
- Ginsburg, R.N., Shinn, E.A., 1994. Preferential distribution of reefs in the Florida Reef Tract: the past is the key to the present. In: Ginsburg, R.N. (Ed.), *Proceedings of the Colloquium on Global Aspects of Coral Reefs: Health, Hazards and History*, pp. 21–26.
- Glaser, K.S., Droxler, A.W., 1991. High production and high-stand shedding from deeply submerged carbonate banks, northern Nicaragua Rise. *J. Sediment. Petrol.* 61, 128–142.
- Glynn, P.W., 1993. Coral reef bleaching: ecological perspectives. *Coral Reefs* 12, 1–17.
- Goldberg, W.M., 1983. Cay Sal Bank, Bahamas: a biologically impoverished, physically controlled environment. *Atoll Res. Bull.* 271, 1–17.
- Grigg, R.W., Epp, D., 1989. Critical depth for the survival of coral islands: effects on the Hawaiian archipelago. *Science* 243, 638–640.
- Halley, R.B., Harris, P.M., 1979. Fresh-water cementation of a 1,000-year-old oolite. *J. Sediment. Petrol.* 49, 969–988.
- Hamilton, P., Larsen, J.C., Leaman, K.D., Lee, T.N., Waddell, E., 2005. Transports through the Straits of Florida. *J. Phys. Oceanogr.* 35, 308–322.
- Harris, P.M., Purkis, S.J., Ellis, J., 2011. Analyzing spatial patterns in modern carbonate sand bodies from Great Bahama Bank. *J. Sediment. Res.* 81, 185–206.
- Haynes, R., Huws, D.G., Davis, A.M., Bennell, J.D., 1997. Geophysical sea-floor sensing in a carbonate regime. *Geo-Mar. Lett.* 17, 253–259.
- Hine, A.C., Steinmetz, J.C., 1984. Cay Sal Bank — a partially drowned carbonate platform. *Mar. Geol.* 59, 135–164.
- Hodell, D.A., Curtis, J.H., Brenner, M., 1995. Possible role of climate in the collapse of Classic Maya civilization. *Nature* 375, 391–394.
- Hoegh-Guldberg, O., 1999. Climate change, coral bleaching and the future of the world's coral reefs. *Mar. Freshw. Res.* 50, 839–866.
- Hoegh-Guldberg, O., Fine, M., Skirving, W., Johnstone, R., Dove, S., Strong, A., 2005. Coral bleaching following wintry weather. *Limnol. Oceanogr.* 50, 265–271.
- Houck, J.E., Buddemeier, R.W., Smith, S.V., Jokiel, P.L., 1977. The response of coral growth rate and skeletal strontium content to light intensity and water temperature. *Proceedings of the 3rd International Coral Reef Symposium*, 2, pp. 425–431.
- Hubbard, D.K., Scaturro, D., 1985. Growth rates for seven scleractinian corals from Cane Bay and Salt River, St. Croix, USVI. *Bull. Mar. Sci.* 36, 325–338.
- Hudson, J.H., 1981. Growth rates in *Montastraea annularis*: a record of environmental change in Key Largo Coral Reef Marine Sanctuary, Florida. *Bull. Mar. Sci.* 31, 444–459.
- Kemp, D.W., Oakley, C.A., Thornhill, D.J., Newcomb, L.A., Schmidt, G.W., Fitt, W.K., 2011. Catastrophic mortality on inshore coral reefs of the Florida Keys due to severe low-temperature stress. *Glob. Chang. Biol.* 17, 3468–3477.
- Kerwin, M.W., Overpeck, J.T., Webb, S.R., DeVernal, A., Rind, D.H., Healy, R.J., 1999. The role of oceanic forcing in mid-Holocene Northern Hemisphere climate change. *Paleoceanography* 14, 200–210.
- Kim, W., Fouke, B.W., Petter, A.L., Quinn, T.M., Kerans, C., Taylor, F., 2012. Sea-level rise, depth-dependent carbonate sedimentation and the paradox of drowned platforms. *Sedimentology*. <http://dx.doi.org/10.1111/j.1365-3091.2012.01321.x>.
- Kindler, P., Mazzolini, D., 2001. Sedimentology and petrography of dredged carbonate sands from Stocking Island (Bahamas). Implications for meteoric diagenesis and aeolianite formation. *Palaeogeogr. Palaeoclimatol. Palaeoecol.* 175, 369–379.
- Kleypas, J.A., Buddemeier, R.W., Gattuso, J.-P., 2001. The future of coral reefs in an age of global change. *Int. J. Earth Sci. (Geol. Rundsch.)* 90, 426–437.
- Kourafalou, V.H., Kang, H.-S., 2012. Florida Current meandering and evolution of cyclonic eddies along the Florida Keys Reef Tract: are they inter-connected? *J. Geophys. Res.* 117, C05028. <http://dx.doi.org/10.1029/2011JC007383>.
- Leaman, K.D., Vertes, P.S., Atkinson, L.P., Lee, T.N., Hamilton, P., Waddell, E., 1995. Transport, potential vorticity, and current/temperature structure across the Northwest Providence and Santaren Channels and the Florida Current off Cay Sal Bank. *J. Geophys. Res.* 100, 8561–8570.
- Lee, Z., Hu, C., Casey, B., Shang, S., Dierssen, H., Arnone, R., 2010. Global shallow-water bathymetry from satellite ocean color data. *EOS Trans. Am. Geophys. Union* 91, 429.
- Lighty, R.G., Macintyre, I.G., Stuckenrath, R., 1978. Submerged early Holocene barrier reef, Southeast Florida shelf. *Nature* 276, 59–60.
- Lighty, R.G., Macintyre, I.G., Neumann, A.C., 1980. Demise of a Holocene barrier-reef complex, northern Bahamas. *Geol. Soc. Am. Abstr. Programs* 12, 471.
- Neumann, A.C., Macintyre, I.G., 1985. Reef response to sea level rise: keep-up, catch-up or give-up. *Proceedings of the Fifth International Coral Reef Congress, Tahiti*, 3, pp. 105–110.
- Newell, N.D., Imbrie, J., Purdy, E.G., Thurber, D.L., 1959. Organism communities and bottom facies, Great Bahamas Bank. *Bull. Am. Mus. Nat. Hist.* 117, 181–228.
- Palmer, M.S., 1979. Holocene facies geometry of the leeward bank margin, Tongue of the Ocean, Bahamas. (MS Thesis) University of Miami, Florida (199 pp.).
- Peterson, L.C., Overpeck, J.T., Kipp, N.G., Imbrie, J., 1991. A high-resolution Late Quaternary upwelling record from the anoxic Cariaco Basin, Venezuela. *Paleoceanography* 6, 99–119.
- Pierson, B.J., 1982. Cyclic sedimentation, limestone diagenesis and dolomitization of upper Cenozoic carbonates of the southeast Bahamas. (Ph.D. thesis) University of Miami, Coral Gables, Florida (343 pp.).
- Pierson, B.J., Shinn, E.A., 1985. Cement distribution and carbonate mineral stabilization in Pleistocene limestones of Hogsty Reef, Bahamas. In: Schneidermann, N., Harris, P.M. (Eds.), *Carbonate Cements*. Special Publications, 36. Society of Economic Paleontologists and Mineralogists, Tulsa, OK, pp. 153–168.
- Purkis, S.J., Pasterkamp, R.J., 2004. Integrating *in situ* reef-top reflectance spectra with Landsat TM imagery to aid shallow-tropical benthic habitat mapping. *Coral Reefs* 23, 5–20.
- Purkis, S.J., Kenter, J.A.M., Oikonomou, E.K., Robinson, I.S., 2002. High-resolution ground verification, cluster analysis and optical model of reef substrate coverage on Landsat TM imagery (Red Sea, Egypt). *Int. J. Remote Sens.* 23, 1677–1698.
- Roberts, H.H., Rouse Jr., L.J., Walker, N.D., Hudson, J.H., 1982. Cold-water stress in Florida Bay and northern Bahamas: a product of winter cold-air outbreaks. *J. Sediment. Petrol.* 52, 145–155.
- Roberts, H.H., Wilson, P.A., Lugo-Fernandez, A., 1992. Biologic and geologic responses to physical processes: examples from modern reef systems of the Caribbean–Atlantic region. *Cont. Shelf Res.* 12, 809–834.
- Rogers, C.S., 1990. Responses of coral reefs and reef organisms to sedimentation. *Mar. Ecol. Prog. Ser.* 62, 185–202.
- Roth, S., Reijmer, J.J.G., 2004. Holocene Atlantic climate variations deduced from carbonate periplatform sediments (leeward margin, Great Bahama Bank). *Paleoceanography* 19, PA1003. <http://dx.doi.org/10.1029/2003PA000885>.
- Schlager, W., 1981. The paradox of drowned reefs and carbonate platforms. *Geol. Soc. Am. Bull.* 92, 197–211.
- Schmitter-Soto, J.J., Comin, F.A., Escobar-Briones, E., Herrera-Silveira, J., Alcocer, J., Suarez-Morales, E., Elias-Gutierrez, M., Diaz-Arce, V., Marin, L.E., Steinich, B., 2002. Hydrogeochemical and biological characteristics of cenotes in the Yucatan Peninsula SE Mexico. *Hydrobiologia* 467, 215–228.
- Smith, N.P., 1995. On long-term net flow over Great Bahama Bank. *J. Phys. Oceanogr.* 25, 679–684.
- Stoessell, R.K., Moore, Y.H., Coke, J.G., 1993. The occurrence and effect of sulfate reduction and sulfide oxidation on coastal limestone dissolution in Yucatan cenotes. *Ground Water* 31, 566–575.
- Stumpf, R.P., Holderied, K., Sinclair, M., 2003. Determination of water depth with high-resolution satellite imagery over variable bottom types. *Limnol. Oceanogr.* 48, 547–556.
- Toscano, M.A., Macintyre, I.G., 2003. Corrected western Atlantic sea-level curve for the last 11,000 years based on calibrated 14C dates from *Acropora palmata* framework and intertidal mangrove peat. *Coral Reefs* 22, 257–270.
- Triffleman, N.J., Hallock, P., Hine, A., 1992. Morphology, sediments, and depositional environments of a small carbonate platform: Serranilla Bank, Nicaraguan Rise, Southwest Caribbean Sea. *J. Sediment. Petrol.* 62, 591–606.
- Veron, J., 1995. *Coral in Space and Time*. University of New South Wales Press, Sydney (321 pp.).

- Veron, J., Minchin, P., 1992. Correlation between sea-surface temperature, circulation patterns and the distribution of hermatypic corals of Japan. *Cont. Shelf Res.* 12, 835–857.
- Weber, M., Lott, C., Fabricius, K.E., 2006. Sedimentation stress in a scleractinian coral exposed to terrestrial and marine sediments with contrasting physical, organic and geochemical properties. *J. Exp. Mar. Biol. Ecol.* 336, 18–32.
- Wilber, R.J., 1981. Late Quaternary history of a leeward carbonate bank margin: a chronostratigraphic approach. (PhD dissertation) University of North Carolina, Chapel Hill, NC (277 pp.).